CHARACTERIZATION OF Tb^{3+}-ACTIVATED BaY_2O_4 PHOSPHORS' FOR OPTOELECTRONICS APPLICATION

Komita SAHU[1], Ravi Shrivastava[2], RAMADHIN, and Siteshwari CHANDRAKAR[3]

The synthesis and photoluminescence analysis of Tb^{3+} doped BaY_2O_4 phosphor was reported in this work. The modified solid state reaction approach, which is best suited for large-scale production, was used to prepare the sample. Scanning Electron Microscopy (SEM), EDS, and X-ray diffraction were used to analyze the produced phosphor sample. The crystallographic information file (mp-3952) was downloaded from material explorer (The material project). The calculated and observed XRD expressed quite significant resemblance hence the crystal structure of the host material considered was reported to be orthorhombic (-P 2ac 2n). The PL emission for the Tb^{3+} doped BaY_2O_4 was detected in the UV-blue areas between 390 and 700 nm. At 273 nm, the excitation spectrum was discovered. There are broad, strong peaks at 490nm, 545nm and 552 nm. The emission in near-white light that is appropriate for white light LED applications is confirmed by the calculate CIE coordinate the near-white emission has a CIE 1931 chromaticity of x = 0.2814, y = 0.2904.Integrated PL Emission Efficiency, Concentration Quenching Efficiency and de-convoluted PL emission peak analysis were done to check the suitability of the phosphor considered in optoelectronic applications.

Keywords: X-ray diffraction, SEM, EDS, CIE coordinate, phosphor, photoluminescence.

1. Introduction

Rare earth ion-doped materials have recently been used to create useful optical devices, including temperature sensors, color display, optical data storage, and biomedical diagnostic[1]. The optical properties of BaY_2O_4 materials, particularly when doped with rare-earth ions like Eu^{3+} and Ce^{3+}, make them highly suitable as hosts in phosphor applications. These materials exhibit favorable luminescent characteristics, including efficient

[1]Department of Physics, Shri Shankaracharya Professional University, BhilaiDurg, Chhattisgarh, India
[2] Department of Physics, GovtGhanshyam Singh Gupt PG collegeBalod, Chhattisgarh, India
[3]Department of Physics, Government VishwanathYadavTamaskar Post Graduate Autonomous College, Durg, Chhattisgarh, India
Corresponding Author (Ramadhin): sahudrrd3@rediffmail.com

excitation and emission spectra, which are critical for applications in solid-state lighting and white light-emitting diodes (LEDs). Ce^{3+} doped BaY_2O_4 emits in the near UV-blue region (350-650 nm), providing versatility in luminescent application[2]. The phosphor exhibits significant excitation peaks at 395 nm and 466 nm, aligning well with the output wavelengths of UV and blue LED chips[3]. Due to its numerous potential uses in automobiles, traffic signals, displays, and general illumination, white light emitters have recently drawn a lot of attention[1]. Combining a blue LED with a fluorescent converter is a more promising way to make white light, even though the output of Red-Green-Blue LEDs can be combined to produce any color, including white[4].

The Tb^{3+} activatedBaY_2O_4 phosphor was synthesized in the current manuscript. The produced phosphor's luminosity study displays a nice photoluminescence (PL) spectrum in white light.

2. Experimental

Experimental for synthesis stoichiometric amounts of the reactant mixture are placed in an alumina crucible and burned in air at 1100ºC for two hours in a muffle furnace to create $BaY_2O_4$with varying concentrations of dysprosium (0.1 to 2.5 mol%). By using modified solid state diffusion at high temperatures, the Tb^{3+} activated BaY_2O_4phosphor was created. Barium oxide (BaO), yttrium oxide (Y_2O_3), Terbium oxide (Tb_2O_3), and boric acid (H_2BO_3) (as a flux) were the initial ingredients high media (99.9%) utilized to construct the sample. To create a uniform powder, the reagent mixture was milled for forty-five minutes. After being moved to an alumina crucible, the powder was heated for four hours at 1350 °C in a muffle furnace. The phosphor materials were allowed to spontaneously cool to normal room temperature[2,5,6]. X-ray diffractions, Scanning Electron Microscopy (SEM) and EDS were used to characterize the samples. The Shimadzu RF-5301 PC spectrofluorophotometer was used to record the excitation and emission spectra of photoluminescence (PL) at room temperature[7,8].

3. Results and discussion

1.1.1. X-ray Diffraction Analysis and crystal structure

The crystallographic information file for the BaY_2O_4 was downloaded from https://next-gen.materialsproject.org/materials and the material ID was mp-3952. The X-ray diffraction pattern for the ideal PL emission concentration

(2.0 mol% of Tb^{3+}) of BaY_2O_4:Tb^{3+}phosphor, was recorded. The calculated XRD for BaY_2O_4 was found using the Software Vesta ver.3.5.7.The stack plot to show the comparison between the positions of prominent peaks present in calculated and observed XRD pattern is provided in Figure 02. The crystal structure (Figure 01) obtained from the said crystallographic information file (cif) was used forRietveld Refinements of the XRD pattern which is shown in Table 3.1[6].

1.1.2. Scanning Electron Microscopy(SEM)

Figure 3.2a shows an image of BaY_2O_4:Tb^{3+} phosphor with an uneven form of agglomerated particles. The borders between the particles and the neighboring ones appear to be melting together due to the apparent hard agglomeration among the particles (Figure3.2b). As we can see in Figure3.2c, the interconnectivity of grain size particles is very well, this is because we prepared the material at high temperature due to which the particles melted well with each other [9,10]. It is clearly seen from Figure3 (a) - Figure3 (c), as the resolving power increases, the size of the particles Figure3(a) - Figure3(c) are 5, 20 and 1 micrometer. Images from SEM of BaY_2O_4: Tb^{3+} phosphors at an ideal (i.e. optimal) concentration of 2.0 mole% are shown in Figure3(a) - Figure3(c), the particles size is estimated to be a few microns, and their surface morphology is slightly rough.

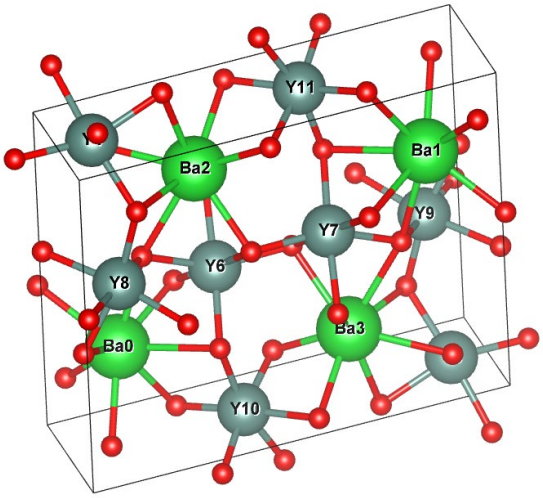

Fig. 01 Crystal structure of un-doped BaY_2O_4

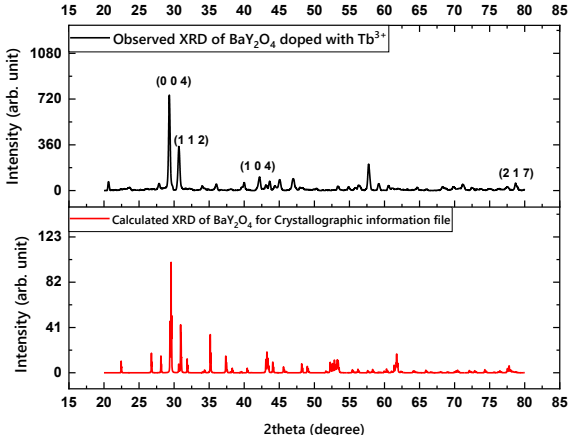

Fig. 02 Comparison between observed and calculated XRD ofBaY_2O_4: Tb^{3+}

Table 3.1:

Lattice parameters refinement results

Zero	Lambda	a	b	c	alpha	beta	gamma	Vol.
0	1.5418	3.46	10.44	12.14	90	90	90	438.5
0	0	1	1	1	0	0	0	

Final values : (Standard errors on 2nd line)

Zero	Lambda	a	b	c	alpha	beta	gamma	Vol.
0	1.5418	3.49	10.6914	12.02	90	90	90	448.5
0	0	0.027	0.1756	0.0892	0	0	0	

h	k	l	2T(Obs)	2T-Zero	2Th(Cal)	Dif
1	1	1	27.88	27.88	27.8968	-0.0168
0	0	4	29.317	29.317	29.7297	-0.4127
1	1	2	30.69	30.69	30.783	-0.093
1	0	4	39.997	39.997	39.575	0.422
1	3	4	47	47	47.3742	-0.3742
0	4	6	57.731	57.731	57.4883	0.2427
1	3	6	59.175	59.175	59.1578	0.0172
2	1	7	78.698	78.698	78.6872	0.0108

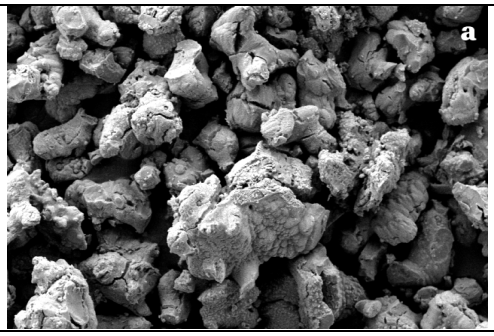

Fig.3(a)SEM images (1k resolution) of

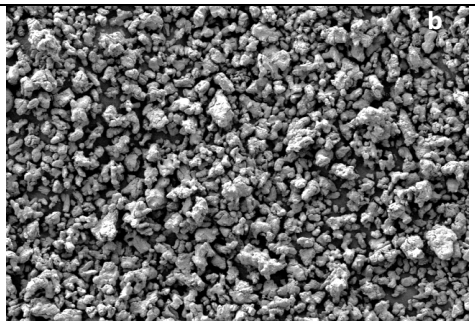

Fig.3 (b)SEM images (5k resolution)

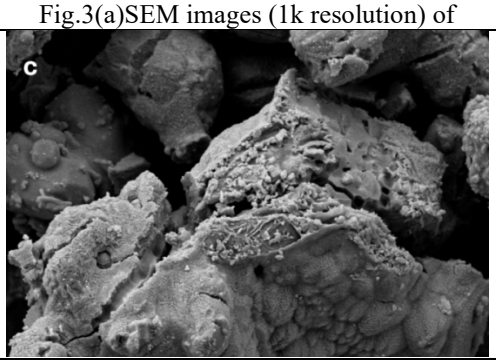

Fig.3 (c)SEM images (15k resolution)

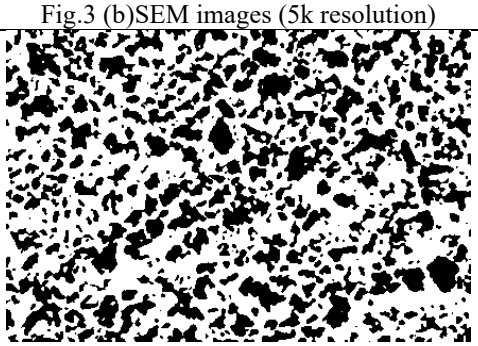

Fig. 3 (d) Threshold image (5k resolution)

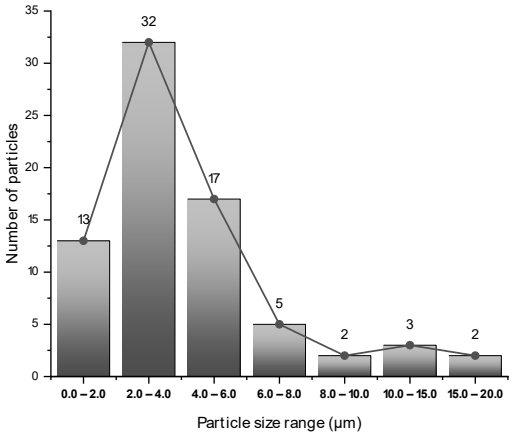

Fig.04 Particle size distribution graph

Particle size distribution analysis was done using software ImageJ v1.53. The particle size distribution graph (Figure 4) obtained from SEM image of the sample recorded in 5k resultion, indicates that the majority of particles exist in the 2–6 µm range, with a dominant size distribution between 2 and 4 µm. The presence of larger particles up to ~20 µm suggests agglomeration, which is commonly observed in solid-state synthesized phosphors. Such microcrystalline morphology is beneficial for reducing surface-related non-radiative defects and contributes to the observed stable photoluminescence behavior[17].

1.1.3. Energy Dispersive X-ray Spectroscopy (EDX)

The elemental composition of the phosphor was determined by EDX spectroscopy (Figure 5). The synthesis of BaY_2O_4: Tb^{3+} phosphor is confirmed by the presence of Tb, Y, B , and O peaks in the spectra. The generated BaY_2O_4:Tb^{3+} phosphor's weight % and atomic percentage were verified by qualitative analysis utilizing the EDX spectra; the results are shown in Table 02

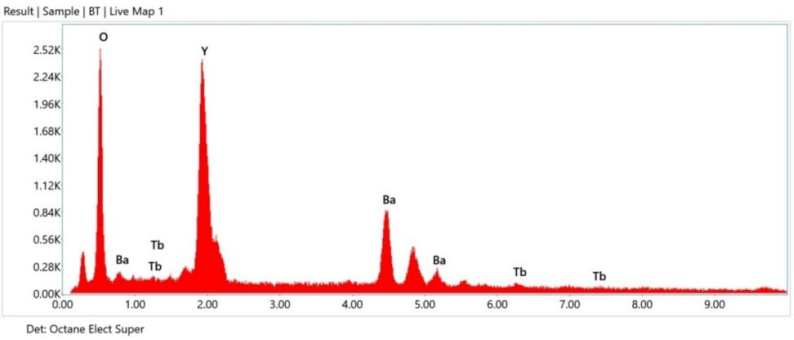

Fig. 05 Elemental composition of the phosphor was determined by EDX spectroscopy

Table 02:

Composition of the elements in SrY_2O_4:Dy^{3+} phosphor

Element	Weight %	Atomic %
O K	16.9	58.4
Y L	37.1	23.1
Ba L	44.7	18.0
Tb L	1.3	0.4

SEM mapping analysis leverages advanced techniques to visualize and quantify the composition of materials at the nanoscale. This process is crucial for various applications, including nanoparticle classification, mineral mapping, and compositional analysis in materials science. Figure 06, shows elemental composition of the phosphor was determined by Mapping Analysis confirmed by the presence of Tb, Y, B , and O gives the capabilities for chemical analysis and chemical mapping on a microscopic scale.[11]

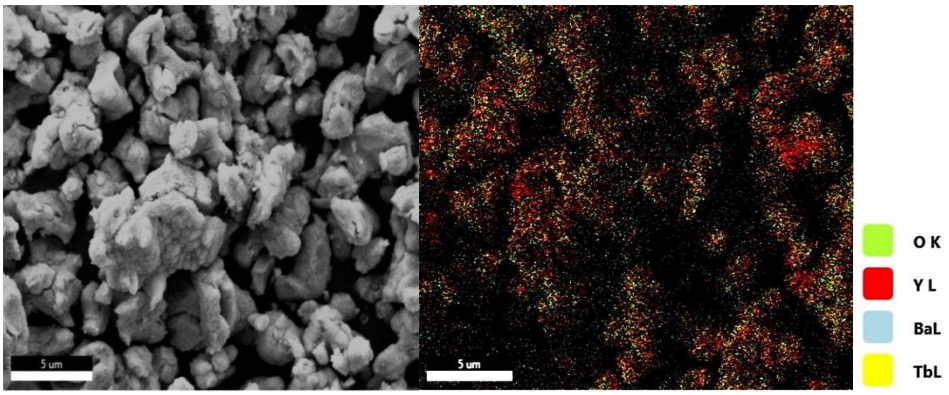

Fig.06 Elemental composition of the phosphor was determined by SEM Mapping Analysis

1.1.4. Photoluminescence (PL) Observation

Figure 07 displays the excitation spectrum of the BaY_2O_4: Tb^{3+} phosphor monitored at 585 nm. The spectrum showed a 273nm, 287 nm and 304nm band transition from $^7F_6 \rightarrow {}^5D_3$ and $^7F_6 \rightarrow {}^5D_4$, which corresponded to the Tb^{3+} ion's intense interactions. As a result, the emission spectra of BaY_2O_4: Tb^{3+} phosphors (Figure 08) show a wide band peak at weak $^5D_4 \rightarrow {}^7F_6$ transitions 490 nm and with a prominent peak at 545nm and 552nm. A prominent intensity band in the emission spectra, located at 545 & 552 nm, is associated with the Tb^{3+} intense Green emission due to a strong $^5D_4 \rightarrow {}^7F_j$ (=5,4) transitions at 545 nm and 552nm transitions[12,13]. Due to its significant spectrum brightness and wide bandwidth, the white light emission of Tb^{3+} in BaY_2O_4 at 490nm, 545nm and 552nm is a suitable choice for the source of light in near white light LED application. Figure 8 shows how dopant concentration affects emission intensity[14]. The intensity of the Tb^{3+} ion concentration increased from 0.5 to 2.0 mol%. However, intensity decreases above 2.0 mol% owing to concentration quenching. According to the findings, Tb^{3+} doped

BaY_2O_4 phosphors might be a useful light source for applications involving optoelectronic devices[15].

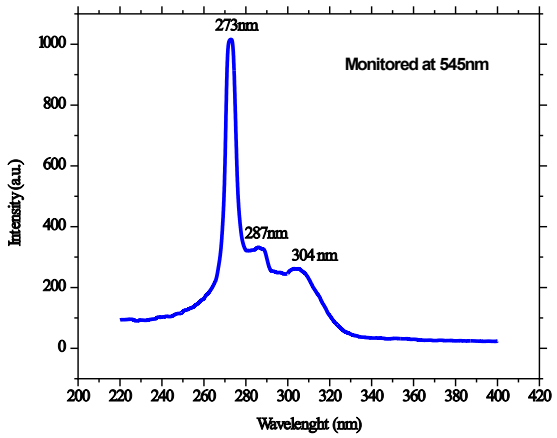

Fig.07 Excitation spectra of the BaY_2O_4: Tb^{3+} phosphor

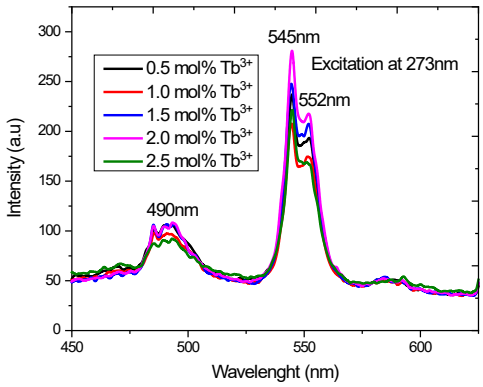

Fig. 08 displays the emission spectra of the BaY_2O_4: Tb^{3+} phosphor at ex = 273 nm

Figure 09 shown The CIE 1931 chromaticity used to calculate CIE coordinate the near-white emission has a CIE 1931 chromaticity of x = 0.2814, y = 0.2904, a correlated color temperature (CCT) of 9796 K, and a color rendering index (CRI) of 89%. This white point is suitable for color-critical display applications due to its extremely high CCT (strongly bluish) which appear as bluer-tinted, cool white[16].

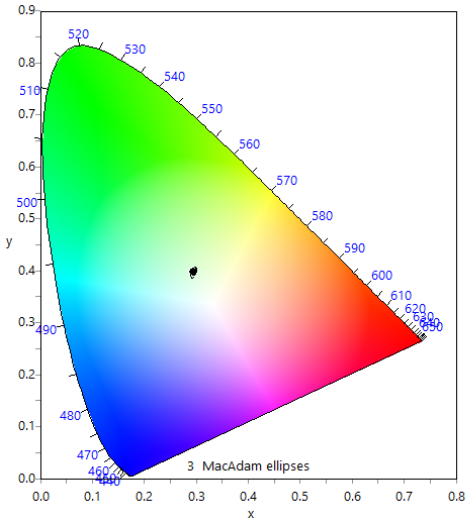

Fig. **09** CIE 1931 chromaticity of the BaY_2O_4:Tb^{3+} phosphor

1.1.5. Integrated PL Emission Efficiency

For finding the PL emission efficiency, area under the graph or Integrated PL was calculated. The data computed for PL spectra is provided in Table (03).

$$I_{int} = \int I(\lambda) d\lambda$$

Table 03

Integrated PL emission

Dopant Concentration	Integrated PL (a. u.)
0.5 mol%	17602.7
1.0 mol%	16812.5
1.5 mol%	17378
2.0 mol%	**17833.9**
2.5 mol%	17767.5

The results (Table 03) indicate that 2.0 mol% dopant concentration represents the optimal composition for achieving maximum integrated PL emission efficiency in the present system. This optimized concentration balances efficient radiative recombination while minimizing non-radiative losses, making it suitable for luminescent and optoelectronic applications.

1.1.6. Concentration Quenching Efficiency

The Quenching efficiency beyond optimum concentration is calculated using the following formula[18]:-

$$\eta_q = \left(\frac{I_{opt} - I_x}{I_{opt}} \right) x100\%$$

Where I_{opt} is integrated PL value for the dopant concentration with optimum emission and I_x is integrated PL value for dopant concentration after optimum PL. The value of n_q was found 0.37% only, which is a very low value. This is an indicative of high structural quality and efficient energy transfer[18].

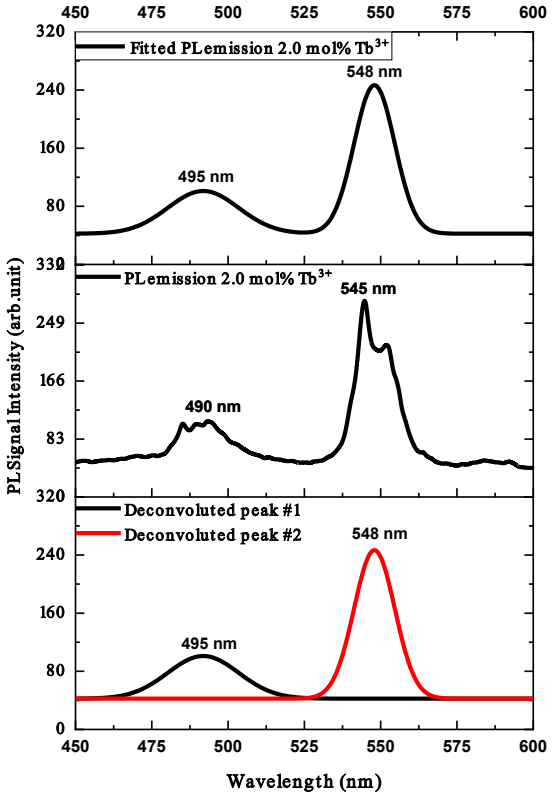

Fig. 10 De-convoluted emission spectrum of BaY_2O_4 doped with 2.0 mol% of Tb^{3+}

The Gaussian deconvolution of the photoluminescence (PL) emission spectrum (Figure 10) reveals the presence of two distinct emission components. A dominant narrow emission peak centered at approximately 548 nm is observed, which is attributed to dopant-centered radiative emission. Such narrow emission features are characteristic of rare-earth doped phosphors and arise from intra-ionic electronic transitions involving shielded 4f electrons, resulting in weak electron–phonon coupling and sharp spectral features.
In addition, a broad emission band located in the 495–505 nm region is identified, which is assigned to host-lattice defect states or charge-transfer-related emission. Broad emission bands of this nature are commonly associated with defect-mediated recombination processes and strong electron–phonon coupling in oxide hosts.

4. Conclusion

The present work offers significant novel information into the properties of BaY_2O_4:Tb^{3+}. The newly synthesized BaY_2O_4: Tb^{3+} was shown to include a orthorhombic crystalline phase by X-ray diffraction examination. Images from SEM of BaY_2O_4: Tb^{3+} phosphor has confirmed the particles size is estimated to be a few microns, and their surface morphology is slightly rough. The PL spectra of the Tb doped BaY_2O_4 phosphor consist of the 4f-4f transitions of elements that are rare earths, which explains why it has a weak peak 490nm and strong 545 & 552 nm peak. However, due to its significant spectrum brightness and wide bandwidth, Tb^{3+} emits white light at 490nm, 574nm and 552 wide spectrum in BaY_2O_4, which makes sense as a light source for while light LED and Display applications. Integrated PL Emission Efficiency, Concentration Quenching Efficiency and de-convoluted PL emission peak analysis were done to check the suitability of the phosphor considered in optoelectronic applications.

REFERENCES

[1] *J. Kovac, L. Peternai,* O. Lengyel, Advanced light emitting diodes structures for optoelectronic applications, Thin Solid Films, Vol. 433, Iss. 1–2, 2003, pp. 22–26.

[2] *V. Dubey, J. Kaur, S. Agrawal,* Effect of europium doping levels on photoluminescence and thermoluminescence of strontium yttrium oxide phosphor, Mater. Sci. Semicond. Process., Vol. 31, 2015, pp. 27–37.

[3] *L. T. Y. Wu,* Synthesis and luminescent properties of red phosphor BaY_2O_4:Eu^{3+} for white light-emitting diodes, Adv. Mater. Res., Vol. 811, 2013, pp. 181–185.

[4] *Y. Li, J. Li, Z. Liu, W. Zhao,* Synthesis and luminescent properties of $BaGd_2O_4:Eu^{3+}$ phosphors with highly efficient red-emitting, J. Rare Earths, Vol. 36, Iss. 8, 2018, pp. 795–801.

[5] *V. Dubey, J. Kaur, N. S. Suryanarayana, K. V. R. Murthy,* Thermoluminescence study including the effect of heating rate and chemical characterization of Amarnath stone collected from Amarnath holy cave, Res. Chem. Intermed., Vol. 40, Iss. 2, 2014, pp. 531–536.

[6] *J. Kaur, R. Shrivastava, V. Dubey, B. Jaykumar,* Kinetics and thermoluminescence glow curve study of $Ba_2MgSi_2O_7:Eu^{3+}$, Dy^{3+}, Res. Chem. Intermed., Vol. 40, Iss. 8, 2014, pp. 2599–2604.

[7] *V. Dubey, R. Tiwari, R. Shrivastava, C. Markande, O. P. Verma, J. Kaur, Y. Parganiha, K. Murthy,* Effect of various cerium ion percentages on photoluminescence and thermoluminescence study of CaY_2O_4 phosphor, J. Display Technol., Vol. 11, 2015, pp. 1–7.

[8] *R. Shrivastava, J. Kaur, V. Dubey, B. Jaykumar,* Photoluminescence, trap states and thermoluminescence decay process study of $Ca_2MgSi_2O_7:Eu^{2+}$, Dy^{3+} phosphor, Bull. Mater. Sci., Vol. 37, Iss. 4, 2014, pp. 925–929.

[9] *W. Strek, P. Dereń, A. Bednarkiewicz, M. Zawadzki, J. Wrzyszcz,* Emission properties of nanostructured Eu^{3+} doped zinc aluminate spinels, J. Alloys Compd., Vol. 300–301, 2000, pp. 456–458.

[10] *R. K. Tamrakar, K. Upadhyay,* Combustion synthesis and luminescence behaviour of Tb^{3+} doped SrY_2O_4 phosphor, J. Electron. Mater., Vol. 47, Iss. 1, 2018, pp. 651–654.

[11] *R. Jones, S. Burgess, P. Pinard,* Enhanced compositional mapping on the SEM through combined EDS–WDS mapping in AZtecWave, Microsc. Microanal., Vol. 28, Suppl. 1, 2022, pp. 546–547.

[12] *T. Dai, G. Ju, Y. Jin, X. Zhou, Y. Li, H. Wu, Z. Hu, Y. Hu,* Novel yellow color-emitting $BaY_2O_4:Dy^{3+}$ phosphors: persistent luminescence from blue to red, Appl. Phys. A, Vol. 126, Iss. 3, 2020, Art. no. 217.

[13] *B. Y. Başaran, V. E. Kafadar, F. M. Emen, E. Öztürk, A. İ. Karaçolak,* Photoluminescence and thermoluminescence studies of beta-irradiated $Ba_3CdSi_2O_8:Tb^{3+}$ phosphor for LED and dosimetry applications, Luminescence, Vol. 40, Iss. 4, 2025, Art. no. e70171.

[14] *S. Liu, Y. Yan, X. Liu, Z. Cui, S. Jia, Y. Xing, S. Guo, B. Wang, Y. Wang,* Concentration quenching inhibition and fluorescence enhancement in Eu^{3+}-doped molybdate red phosphors with two-phase mixing, RSC Adv., Vol. 13, Iss. 44, 2023, pp. 31167–31175.

[15] *V. Singh, P. Rohilla, S. Kaur, A. S. Rao,* Tb^{3+} activated $Na_3YSi_2O_7$ phosphors for display panels, Optik, Vol. 271, 2022, Art. no. 170221.

[16] *T. Ghosh, E. Prasad,* White-light emission from unmodified graphene oxide quantum dots, J. Phys. Chem. C, Vol. 119, Iss. 5, 2015, pp. 2733–2742

[17] *P, Dorenbos,* Energy of the first 4f–5d transition of Ce^{3+} in inorganic compounds, Journal of Luminescence, Vol. 104, 2003, pp. 239–260

[18] *D. L. Dexter,* A theory of sensitized luminescence in solids, Journal of Chemical Physics, Vol. 21, 1953, pp. 836-850